Journal of Oceanography, Vol. 63, pp. 349 to 362, 2007

Utility of an Automatic Water Sampler to Observe Seasonal Variability in Nutrients and DIC in the Northwestern North Pacific

MAKIO C. HONDA* and SHUICHI WATANABE

Japan Agency for Marine-Earth Science and Technology, Natsushima, Yokosuka, Kanagawa 237-0061, Japan

(Received 14 September 2006; in revised form 17 November 2006; accepted 24 November 2006)

Concentrations of nutrients (NO_3, NO_2, $Si(OH)_4$, PO_4) and dissolved inorganic carbon (DIC) were measured in a series of seawater samples collected over approximately 15 months in 2005 and 2006 by an automatic water sampler (Remote Access Sampler, RAS) in the Northwestern North Pacific. Seasonal variability and concentrations of $NO_3 + NO_2$ (NO_x) and $Si(OH)_4$ were comparable to previous shipboard observations, although there were small errors associated with measurements of PO_4 and DIC. Concentrations of these nutrients began to decrease in late April. After the end of June, NO_x and $Si(OH)_4$ decreased rapidly, with large fluctuations. After October, these nutrients increased again until late spring 2006. The ratio of the decrease of $Si(OH)_4$ to that of NO_x suggests that numbers of biogenic opal-producing creatures, such as diatoms, increased after the end of June. This conclusion was supported by a rapid increase in biogenic opal flux recorded in a sediment trap at 150 m. The relationship between NO_x concentrations at the RAS depth of 35 m and NO_x integrated over the upper 100 m was determined using previous shipboard hydrocast data. This relationship was used to estimate integrated mixed layer NO_x concentration from RAS data. Estimated new production based on seasonal drawdown of integrated NO_x averaged approximately 156 mg-C $m^{-2}day^{-1}$ annually, which agrees with previous estimates. Thus, an automatic seawater sampler that documents annual maximum and minimum nutrient concentrations and episodic events such as storms and spring blooms, which might be missed by an ordinary research vessel, will contribute to time-series observations of nutrients and, by extension, biological pump activity.

Keywords:
· Time-series observation,
· mooring system,
· automatic water sampling,
· nutrients,
· biological pump.

1. Introduction

Biological activity in the ocean plays an important role in the uptake of atmospheric CO_2, which is increasing due to anthropogenic activity. The processes of assimilation (primary production), calcification, and transport of carbon to the ocean interior are referred to as the biological pump (Volk and Hoffert, 1985; Sarmiento and LeQuere, 1996; Falkowski *et al*., 1998; Sigman and Boyle, 2000). This mechanism is influenced by ambient physical, chemical, and biological conditions. Recently, changes in the biological pump due to global warming, and the pump's positive or negative feedback to global warming have been of great concern (e.g., Heinze, 2004; Orr *et al*., 2005). However, these changes can be detected only by long-term observations. It is therefore apparent that time-series observations are necessary and much effort has been expended on conducting time-series observations in the world ocean, for example, in the subtropical Pacific (Station ALOHA; Karl *et al*., 1996, 2001), the middle Atlantic (Station BATS; Dickey *et al*., 2001), and the Eastern North Pacific (Station OSP; Harrison *et al*., 1999, 2004).

These time-series studies show that frequent observations (at least monthly) are required for a better understanding of the ocean's role in the uptake of atmospheric CO_2. However, conducting high frequency observations, especially during the winter season at high latitudes, is difficult with ordinary research vessels. Observations using automatic samplers or automatic sensors on mooring systems have allowed time-series observations of seasonal variability in the biogeochemistry with high sampling frequency (e.g., Dickey *et al*., 1998), allowing the

* Corresponding author. E-mail: hondam@jamstec.go.jp

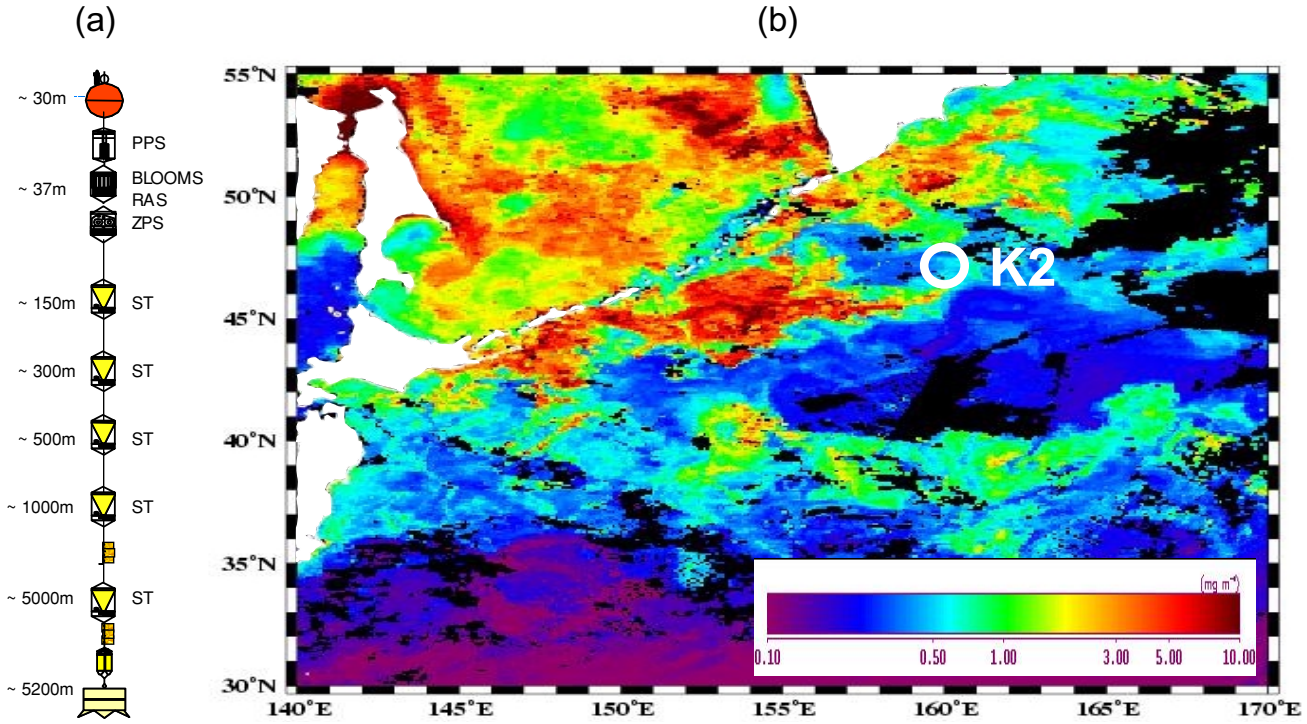

Fig. 1. (a) Mooring system. PPS, phytoplankton sampler; BLOOMS, Bio-optical Long-term Optical Ocean Measuring System; RAS, automatic water sampler; ZPS, zooplankton sampler; ST, sediment trap. Data from BLOOMS, PPS, ZPS and ST are not presented in this paper. (b) Location of station K2. Color image shows SeaWiFS Chlorophyll-*a* monthly composite in June 2005 (courtesy of K. Sasaoka, JAMSTEC).

observation of episodic events such as sudden increases of biological pump activity caused by meteorological disturbances and the spring bloom.

The time-series sediment trap has been one of the more effective samplers for the time-series study of the biological pump (e.g., Honjo, 1996; Conte *et al.*, 2001, 2003). However, sediment traps have usually been deployed in the deep ocean (below 1000 m) to avoid biological and hydrodynamic disturbances, and there is concern about how well deep sediment trap data reflect biological activity in the upper ocean layer and the behavior of sinking particles in the mesopelagic layer, or "twilight zone." Recently, remote sensing technology for oceanography (satellite oceanography) has advanced and large-scale time-series observation has become possible (Banse and English, 1999; Campbell *et al.*, 2002; Behrenfeld *et al.*, 2005; Dickey *et al.*, 2006). However, remote sensing provides data primarily about physical conditions and biological activity near the sea surface. In addition, the existence of clouds often hampers acquisition of satellite ocean color data, especially in coastal and high-latitude regions. To clarify how much carbon is assimilated in the upper ocean and transported to the ocean interior, time-series observations in the surface euphotic zone or mixed layer are required.

Since 2001 we have been conducting time-series observations in the Western North Pacific using a mooring system (Fig. 1(a)). This system consists of automatic samplers such as sediment traps (between the subsurface layer and the deep ocean), phytoplankton and zooplankton samplers, and an optical sensor (in the euphotic layer; <50 m). An automatic water sampler, called a Remote Access Sampler (RAS), has also been installed on the mooring system to collect seawater samples for the measurement of nutrients and dissolved inorganic carbon (DIC), which are good indicators of the biological pump. Although automatic water sampling systems have been developed previously (e.g., Bell *et al.*, 2002), there have been few reports that document time-series observations of nutrients and DIC in the pelagic ocean. This study presents preliminary results on seasonal variability in nutrients and DIC observed by our automatic water sampler and the potential of the automatic sampler for the study of the biological pump is introduced.

2. Materials and Methods

2.1 Description of the study area

A bottom-tethered mooring system was deployed at station K2 (47°N, 160°E, water depth 5280 m). Its posi-

tion was selected after a geographic bottom survey with a multi-channel, narrow beam echo sounding system (SeaBeam 2112.004), which was used to find a flat sea floor with a few miles radius, and an altimeter (Datasonics PSA900D) attached below a multiple water sampling system with CTD to determine the precise water depth. Details of the geographic survey and mooring work have been described elsewhere (Idai *et al*., 2005; Honda, 2005).

Station K2 is located in the North Pacific Western Subarctic Gyre (WSG). The WSG has large seasonal variability in physical, chemical, and biological parameters (reviewed by Harrison *et al*., 2004). Surface water temperatures range from approximately 1°C in winter to over 10°C in summer and mixed-layer depth (MLD) ranges from a maximum of 150 m in winter to approximately 20 m in summer. In late spring, primary productivity increases with temperature, light intensity, and water stratification. Seasonal drawdown of nutrients and DIC from late winter to early autumn is greater than in other oceans (Tsurushima *et al*., 2002). However, nutrients are not depleted even in late summer or early autumn. The euphotic layer is relatively constant, extending to approximately 50 m depth (Imai *et al*., 2002) and diatoms numerically predominate in the phytoplankton assemblage throughout the year (Mochizuki *et al*., 2002).

High biological pump activity is suspected based on large seasonal changes in nutrient concentrations (Launchi and Najjar, 2000) and pCO_2 (Takahashi *et al*., 2002). Station KNOT is a well-known time-series station in the WSG (see special issue of *Deep-Sea Research II*, **49**, Nos. 24–25). Between 1998 and 2001, a comprehensive study was conducted at station KNOT (44°N, 155°E) and some unique characteristics were reported, such as large seasonal variability in nutrients and carbonate species (Tsurushima *et al*., 2002) and a high organic carbon transfer efficiency (Honda *et al*., 2002). However, the data did not always represent oceanographic conditions in the WSG since station KNOT is located at the southeastern boundary of the WSG and is sometimes influenced by subtropical and coastal water. We selected station K2 to succeed station KNOT. At station K2, time-series observations by both our moored system and the R/V *MIRAI* have been conducted since 2001. In addition, a scientific cruise that focused on comparison of the biological pump at station K2 with that at station ALOHA was conducted in 2005 by the VERtical Transport In the Global Ocean (VERTIGO) project group (Buesseler *et al*., 2006; http://cafethorium.whoi.edu/).

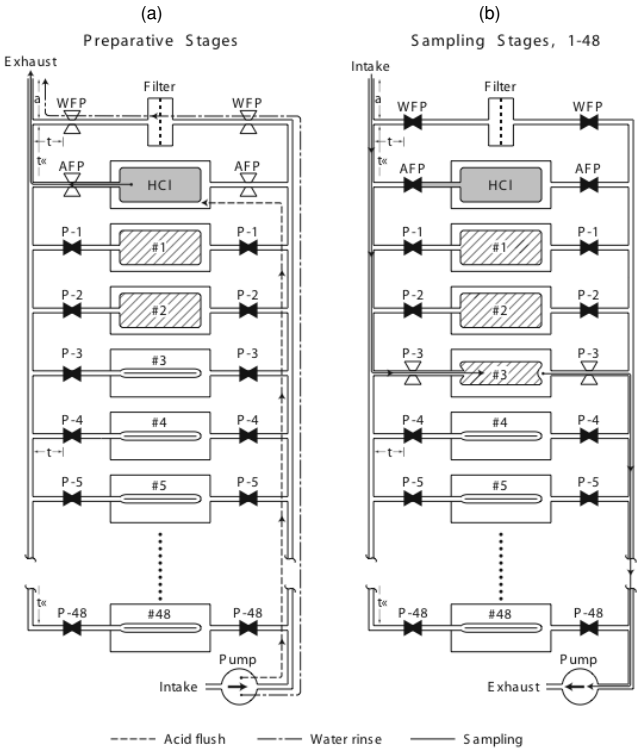

Fig. 2. Functional diagram of the Remote Access Sampler (RAS) (courtesy of S. Honjo). During the preparative stage ((a) left panel) the RAS executes two functions in order to avoid contamination from biofouling along the intake path "a" (upper-left corner). First, through the acid flush path, a pair of AFP (Acid Flush Path) valves opens and a pump applies pressure to a sample bag containing HCl that flushes the intake manifold "a" and then closes the AFP valves to isolate the HCl bag. Second, WFP (Water Flush Path) valves open in the water rinse path and filtered *in situ* seawater is pumped to rinse out any remaining HCl from "a". WFP valves then close. The RAS is then ready for water sampling through the sampling path ((b) right panel). Microprocessor commands open twin valves of the next empty bag, pre-loaded with a preservative (bag P-3, for example). The pump runs in reverse to generate a lower pressure in the sheath holding the sample bag, resulting in the drawing in of *in situ* seawater of programmed volume. The bag is then isolated for preservation by closing valves P-3 until the next programmed cycle that starts with HCl flushing. In an actual RAS, all valves are arranged along two circumferences and virtual manifolds "t" and "t <<" do not exist.

2.2 *Description of automatic water sampler*

We automatically collected time-series water samples using a Remote Access Sampler (RAS; McLane RAS 3-48-500). The RAS uses a pump to draw water out of an acrylic sample container in which a collapsed sample bag is mounted (Fig. 2). This creates a pressure gradient that pushes ambient seawater through the intake and into the inflating sample bag. The 500 ml capacity sample bags are made of three laminated layers: a thin exterior Mylar® film for protection, a vacuum-coated aluminum-foil layer to block solar radiation and minimize gas diffusion, and

Table 1. Results from test of preservation method for nutrients and DIC in RAS samples. For comparison, ordinal hydrocast data are also shown. All data are normalized to salinity of 33.

	Hydrocast	RAS sampling		
Sampling date	04-Mar-05	07-Mar-05	07-Mar-05	07-Mar-05
Analysis date	04-Mar-05	18-Mar-05	04-Oct-05	23-Jun-06
Sample number	2	6	2	2
N-DIC (μmol kg^{-1})	2120.93 ± 4.88	2129.46 ± 4.89	2120.07 ± 4.89	2123.53 ± 7.15
N-NO_3 (μmol kg^{-1})	23.03 ± 0.12	23.82 ± 0.12	23.72 ± 0.12	23.26 ± 0.10
N-NO_x (μmol kg^{-1})	23.16 ± 0.12	23.97 ± 0.12	23.89 ± 0.12	23.50 ± 0.10
$Si(OH)_4$ (μmol kg^{-1})	40.86 ± 0.20	41.08 ± 0.20	41.74 ± 0.20	41.13 ± 0.49
PO_4 (μmol kg^{-1})	1.89 ± 0.01	1.90 ± 0.01	1.92 ± 0.01	1.90 ± 0.00

an inner Teflon® film for reinforcement and insulation of the sample water from the aluminum-foil layer. Each bag was pre-loaded with an $HgCl_2$ preservative solution (see Subsection 2.3), connected to a distribution valve and placed within a rigid acrylic 600 ml sample bag container, or sheath. Before deployment, the space surrounding the sample bag within each sheath was filled with filtered surface seawater with salinity adjusted to approximately 40 by the addition of NaCl. We employed saline water with higher density rather than pure water with lower density than ambient seawater because there was a possibility that exhausted pure water during seawater sampling might ascend from the outlet at the lower part of the RAS (Exhaust in Fig. 2(b)) and contaminate seawater sampled from the inlet at the upper part of the RAS (Intake in Fig. 2(b)). Each RAS held 49 identical bag assemblages. Of these, 48 were used to sample seawater in a scheduled sequence at programmed event times. The remaining bag was filled with 6 M HCl that was used to flush the seawater intake path before each water sampling event to prevent biofouling. After flushing with HCl, the intake path was flushed with ambient seawater and then seawater samples of approximately 500 ml were collected. Execution records documenting sample timing, estimated sample volume, flushing periods, and electricity consumption were logged by the RAS instruments and retrieved from the memory after recovery.

The mooring system with RAS was deployed and recovered twice during this study; the first deployment was from March 2005 to September 2005 (phase I) and the second deployment from October 2005 to May 2006 (phase II). The RAS was initialized to collect *in situ* seawater samples at 4-day intervals from 20 March 2005 to 29 May 2006 (436 days), except between 20 December 2005 and 11 April 2006, when the sampling interval was 8 days. This produced 94 seawater samplings, although several samplings failed due to accidental disconnection of the suction tube or loss of the acrylic sheath with the sample bag.

2.3 Preservation of samples

We used a mercuric chloride ($HgCl_2$) solution as a preservative. Before deployment, 2 ml $HgCl_2$ solution (36,000 ppm; 3.6 g $HgCl_2$ in 100 ml distilled water) was pre-loaded in each sample bag. In a seawater sample of approximately 500 ml, the final concentration of $HgCl_2$ was approximately 140 ppm. This $HgCl_2$ concentration is comparable to that used for long-term preservation of seawater samples for measurement of nutrients (105 ppm; Kattner, 1999) and approximately 15 times higher than that used in the measurement of carbonate species (approximately 10 ppm; DOE, 1994).

During the R/V *MIRAI* cruise MR05-01 in March 2005, we collected seawater samples by RAS and tested the effectiveness of the preservation method for nutrient and DIC samples. We added $HgCl_2$ solution to 500 ml seawater samples, as described above, and measured concentrations of nutrients and DIC when seawater samples were first collected (March 2005), after 6 months (September 2005), and after 15 months (June 2006). Samples were stored in a refrigerator at 4°C between analyses. We found good agreement between all three sets of measurements: within 2% for nutrients and 0.2% for DIC (Table 1). Thus we determined that the chosen concentration of preservative was appropriate for these observations.

2.4 Sampling depth, temperature, and salinity

The depth of the RAS was measured every 120 min during mooring deployment using a depth sensor (RIGO RMD-500). Water temperature at the RAS depth was deduced by a thermistor inside the RAS electronics pressure housing. This thermistor recorded the temperature inside the RAS housing when seawater sampling started and stopped for each sample. The initial temperature reading should have represented the environmental temperature since at least 4 days would have passed since the previous sampling, although its accuracy is ±0.5°C, it cannot detect low temperatures (<2°C), and the temperature usually increased by up to 2–3°C by the end of sam-

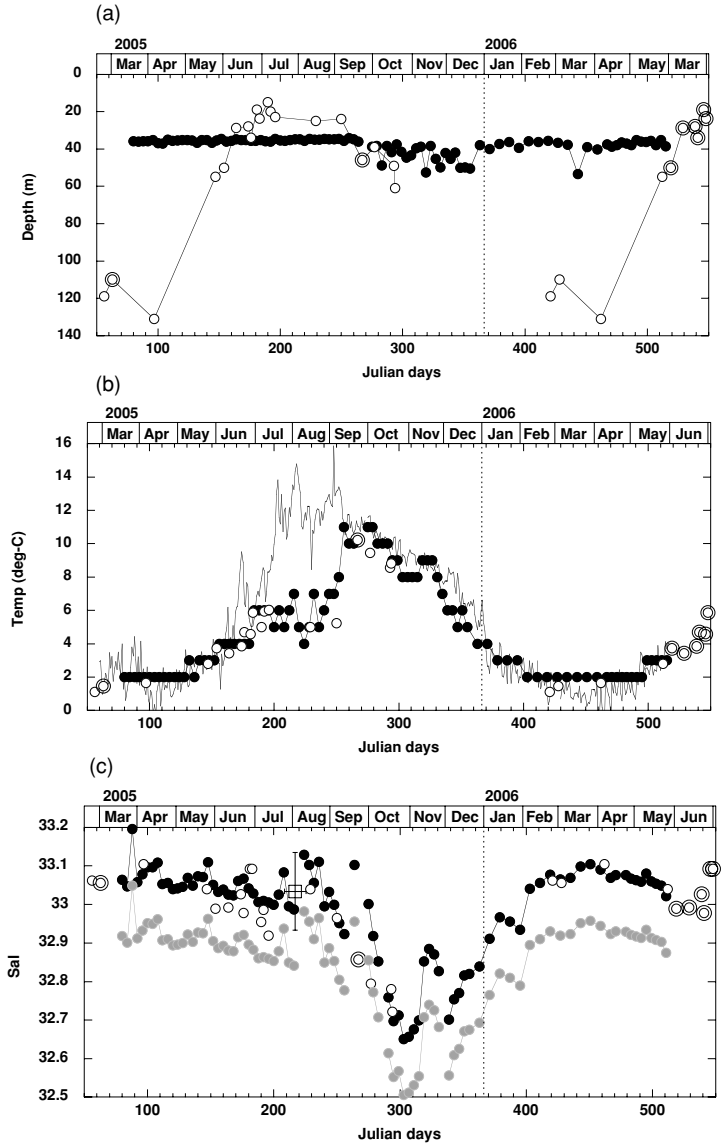

Fig. 3. (a) Seasonal variability in RAS sampling depths (closed circles), and the mixed layer depths (MLD) based on hydrocast data (double circles) and climatological data (open circles) (see text). RAS sampling depths are depths at which respective seawater samplings were conducted. Horizontal axis is Julian days (JD). JD 1 and JD 367 are 1 January 2005 and 1 January 2006, respectively. (b) Seasonal variability in *in situ* temperature observed by RAS thermistor (closed circles), and water temperature at 35 m based on hydrocast data (double circles) and climatological data (open circles) (see text). Solid line indicates Sea Surface Temperature (SST) obtained by satellite (courtesy of K. Sasaoka, JAMSTEC). (c) Seasonal variability in salinity of RAS samples. Gray circles are observed salinities and closed circles are salinities corrected for dilution of RAS sample mainly by preservative. Double circles and open circles show hydrocast and climatological data, respectively. A square with cross is a mean VERTIGO salinity data value (see text). Vertical error bar is standard deviation (1σ) of VERTIGO salinity data (n = 26) and horizontal error bar is period when VERTIGO data were obtained.

pling.

The salinities of RAS samples were measured onboard by an inductively coupled salinometer (AutoLab®: YEO-KAL) after recovery. Based on replicate analysis, measurement error was 0.02 on average.

2.5 Nutrients and DIC

After recovery, each RAS water sample was subdivided into four aliquots for onboard analysis of DIC, nutrients, salinity, and other biogeochemical constituents (not included in this article).

Nutrient concentrations [(NO_x (NO_2 + NO_3), $Si(OH)_4$ and PO_4] were measured with an onboard continuous flow analytical system (BRAN+LUEBEB TRAACS® 800) following the procedures described by Aoyama (2005). The efficiency of the copperized-cadmium reductor (Cu-Cd column) used in nitrate analysis was checked frequently because of accelerated loss of efficiency resulting from $HgCl_2$ in the samples.

PO_4 concentrations could not be determined in approximately 20% of the samples (18 out of 89) due to color-dulling of the phosphomolybdous acid produced in the molybdenum blue method (Murphy and Riley, 1961).

For DIC analysis, sample water was introduced directly from the sampling bag assemblage into a DIC extraction module with a CO_2 coulometer (Ishii *et al.*, 1998) by applying a gentle N_2-gas pressure to the sheath cavity.

The variabilities (deviations from the mean) in analyses from six replicate RAS samples collected at 6 hour intervals were 0.40, 0.33, 0.002, and 2.9 μmol kg^{-1} for NO_x, $Si(OH)_4$, PO_4, and DIC, respectively. Analytical errors, based on replicate analyses of reference materials, were less than 0.09, 0.19, 0.004, and 1.1 μmol kg^{-1} for NO_x, $Si(OH)_4$, PO_4 (n = 10), and DIC (n = 27), respectively.

3. Results

The results obtained from RAS samples in this study were validated by comparison with two other sets of data (Figs. 3 and 4). Hydrocast data were collected at 35 m depth at station K2 during the cruises that deployed and recovered the mooring system and RAS. Climatological data from other cruises conducting hydrocasts at station K2 from 2001 to 2006 were also used for comparison (http://www.jamstec.go.jp/mirai/). In addition, the VERTIGO cruise (R/V *ROGER REVELLE*) was being conducted during mooring deployment (30 July to 15 August 2005) near station K2 (between 46.1°N and 47.9°N and 158.67°E and 161.32°E) and the unpublished data obtained during the cruise from 35 m at 26 stations were used for comparison (courtesy of K. Buesseler and P. Henderson, Woods Hole Oceanographic Institution).

3.1 Water depth, temperature, and salinity

3.1.1 Water depth

The RAS sampling depth increased slightly from March to September 2005 (Fig. 3(a)). This might be attributed to a decrease of current velocity resulting in less tilt of the mooring system or greater stretching of the mooring wire ropes during deployment. However, the RAS sampling depths were very stable during phase I, with an average of 35.4 ± 0.6 m (mean ±1σ) and a range from 34.2 to 37.1 m (Table 2). During phase II, RAS depths showed greater variation, ranging from 35.3 to 53.5 m with an average of 40.5 ± 5.0 m (mean ±1σ). The surface mixed-layer depths (MLD) shown in Fig. 3(a) were defined with 0.125 criteria, that is, a depth with density (sigma theta) of 0.125 higher than that at surface, based on hydrocast and climatological data. The maximum MLD was in March (approximately 140 m) and the minimum

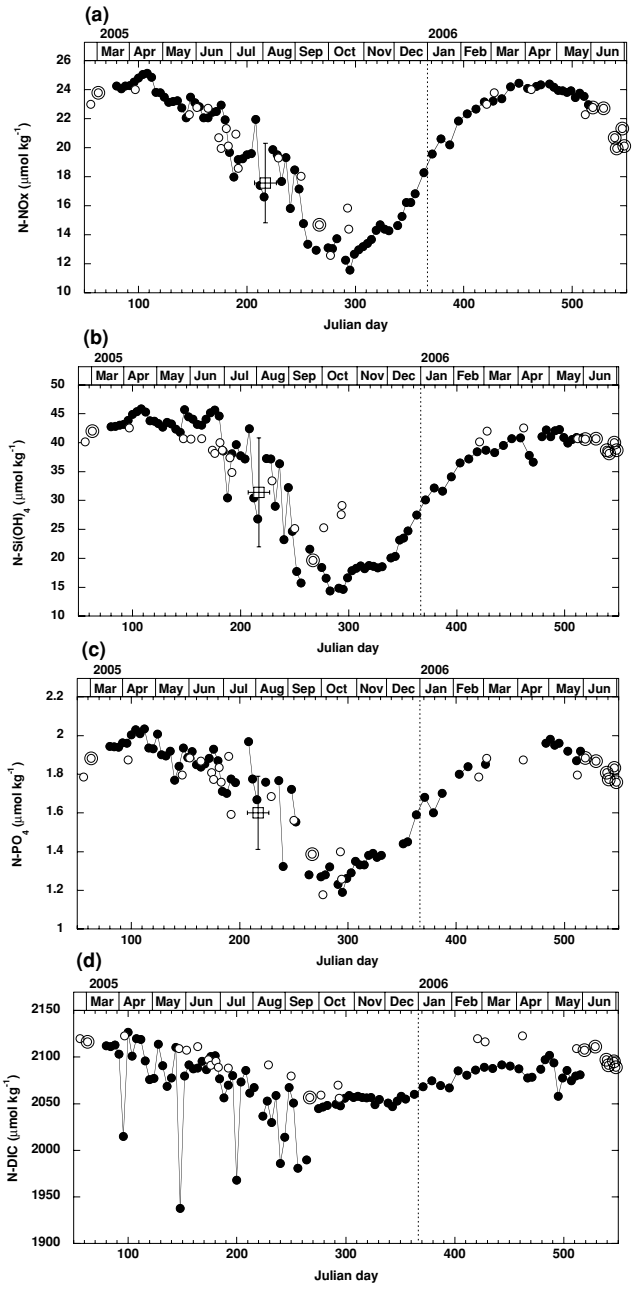

Fig. 4. Seasonal variability in (a) NO_x, (b) $Si(OH)_4$, (c) PO_4, and (d) DIC. Closed circles, open circles and double circles show observed data from RAS, climatological data and hydrocast data, respectively. A square with cross is VERTIGO data value, with standard deviation. All data are normalized to a salinity of 33.

was in July (approximately 20 m). Based on seasonal changes in the MLD, we believe that the RAS was located in the mixed layer throughout the year, except for the period between mid-June 2005 to late September 2005.

3.1.2 Water temperature

Water temperature at RAS depth (i.e., *in situ* water temperature) was approximately 2°C by early May 2005 (Julian day (JD) 128; Table 2, Fig. 3(b)). Thereafter, *in situ* water temperatures increased with some fluctuation to the annual maximum of approximately 11°C in September and October 2005. Temperatures then decreased until February 2006 and increased again beginning in May 2006. The seasonal variability of *in situ* temperature observed in this study coincided well with hydrocast and climatological temperature data. Compared to sea surface temperature (SST) around station K2, as observed by the Advanced Very High Resolution Radiometer (AVHRR) sensor aboard satellite NOAA, *in situ* temperature was substantially lower than SST between early June 2005 and late September 2005, while *in situ* temperature generally agreed with SST during other periods. This evidence supports the conclusion that the RAS was located in the surface mixed layer throughout the year except for the period between early June and late September 2005.

3.1.3 Salinity

Salinity values had wide fluctuations, but generally tended to be higher during winter and lower in autumn, with trends similar to those evident in hydrocast and climatological salinity data (Fig. 3(c)). RAS salinities were approximately 0.2 lower than hydrocast and climatological values. This resulted from the dilution of RAS samples by preservative (2 ml $HgCl_2$ solution), while the actual dilution factor depended on the seawater sample volume. If the RAS seawater sample volumes were exactly 500 ml, RAS samples were diluted by 0.4%. Taking this dilution into account, observed RAS salinity data were corrected (closed circles in Fig. 3(c)). Corrected salinity generally coincided with hydrocast, climatological, and VERTIGO salinity data, ranging from approximately 32.6 to 33.1. As the VERTIGO salinity data, which have large fluctuation, show, salinity is expected to be variable at 35 m at station K2 in summer.

3.2 Nutrients and DIC

The following nutrient and DIC data were normalized to a constant salinity of 33 to correct for the dilution of the RAS seawater sample by the addition of 2 ml preservative, and to eliminate the effects of natural evaporation and precipitation. For comparison, hydrocast, climatological, and VERTIGO data were also normalized to a salinity of 33.

3.2.1 NO_x

We observed maximum NO_x (NO_3 + NO_2) concentrations, normalized to a salinity of 33 (N-NO_x), in the middle of April 2005 (JD 108; Table 2 and Fig. 4(a)). After that, N-NO_x concentrations decreased. The decrease after the end of June (JD 180) was particularly large and was accompanied by large fluctuations. These fluctuations might have occurred because the RAS was located just below the mixed layer where a steep vertical gradient in N-NO_x concentrations resulted in variable RAS nutrient data. The annual minimum N-NO_x was observed in late October 2005 (JD 295). Based on climatological N-NO_x data and previous reports (Wong *et al*., 2002a, b), this minimum value of approximately 11 μmol kg^{-1} was comparable to the annual minimum value observed in surface water, although the surface water minimum generally appears in summer. Thus, the RAS could have observed the surface nutrient minimum, although the RAS depth was slightly below the mixed layer during July and September. N-NO_x concentrations increased again toward the middle of April 2006 (JD 478). Seasonal variability in N-NO_x was comparable to that of hydrocast and climatological data. In addition, our data from July and August 2005 were comparable to those obtained by the VERTIGO research group in July and August 2005, which also showed large fluctuations in N-NO_x concentrations near station K2 at 35 m depth.

3.2.2 $Si(OH)_4$

Concentrations of normalized $Si(OH)_4$ [N-$Si(OH)_4$] also increased by mid-April 2005 and then decreased (Fig. 4(b)). However, unlike N-NO_x, N-$Si(OH)_4$ maintained high concentrations through the end of June (JD 180) and the annual maximum concentration was observed during this period. After that, N-$Si(OH)_4$ concentrations decreased substantially until the middle of October 2005 (approximate JD 280) with fluctuations similar to N-NO_x. After mid-October 2005, N-$Si(OH)_4$ increased again toward April 2006 (JD 478). Seasonal variability in N-$Si(OH)_4$ coincided with that of hydrocast and climatological data. In addition, N-$Si(OH)_4$ in RAS samples coincided well with VERTIGO N-$Si(OH)_4$ data within its variability.

3.2.3 PO_4

Concentrations of PO_4 could not be determined for approximately 20% of the total samples, as described in Subsection 2.5 (see also Discussion, Subsection 4.1), but normalized PO_4 (N-PO_4) concentrations from the remaining samples showed the same seasonal patterns as N-NO_x: a decrease from April 2005 to October 2005 with fluctuations and an increase again to April of 2006 (Fig. 4(c)). Seasonal variability agreed with hydrocast, climatological, and VERTIGO data. The ratio of changes in N-NO_x and N-PO_4 concentrations ($\Delta N/\Delta P$) was approximately 16, a ratio consistent with the phytoplankton N/P uptake ratio reported previously (Redfield *et al*., 1963; Anderson and Sarmiento, 1994).

The correlation between salinity and nutrient con-

Table 2. Depths, *in situ* temperatures, salinities, nutrients and DIC for RAS samples during phase I and phase II. S/N is sample number. Experimental day numbers start with first RAS sampling on 20 March 2005, which was also Julian day (JD) 80. 1 January 2006 is expressed as JD 367 in this study. N.S. and N.D. indicate no sample and no data, respectively.

(Phase I) Deployment date: 17-Mar-05; Recovery date: 22-Sep-05; Position: 47°01′ N, 159°57′ E; Water depth: 5206 m

S/N	Sampling date	Experimental days	Julian days	RAS depth (m)	Water temp. (deg-C)	Salinity	NO_3 (μmol kg^{-1})	NO_x (μmol kg^{-1})	$Si(OH)_4$ (μmol kg^{-1})	PO_4 (μmol kg^{-1})	DIC (μmol kg^{-1})
1	20-Mar-05	1	80	35.8	2	32.918	24.01	24.20	42.68	1.94	2106.8
2	24-Mar-05	5	84	36.0	2	32.901	23.80	23.99	42.67	1.94	2104.8
3	28-Mar-05	9	88	35.8	2	33.049	24.10	24.29	43.13	1.94	2116.4
4	01-Apr-05	13	92	35.9	2	32.912	24.01	24.21	43.08	1.96	2097.5
5	05-Apr-05	17	96	35.3	2	32.932	24.29	24.49	43.79	1.96	2010.6
6	09-Apr-05	21	100	36.8	2	32.951	24.57	24.78	44.85	2.00	2123.7
7	13-Apr-05	25	104	37.1	2	32.950	24.81	25.01	45.34	2.03	2097.9
8	17-Apr-05	29	108	35.0	2	32.962	24.89	25.11	45.79	2.01	2117.4
9	21-Apr-05	33	112	35.7	2	32.907	24.54	24.79	45.16	2.03	2113.0
10	25-Apr-05	37	116	35.4	2	32.910	23.51	23.77	43.70	1.93	2090.2
11	29-Apr-05	41	120	35.3	2	32.894	23.43	23.71	43.56	1.92	2069.2
12	03-May-05	45	124	35.1	2	32.896	23.12	23.42	43.18	2.00	2070.6
13	07-May-05	49	128	35.5	2	32.900	22.79	23.05	42.55	1.90	2107.3
14	11-May-05	53	132	36.7	3	32.922	22.88	23.15	43.39	1.89	2085.7
15	15-May-05	57	136	35.3	2	32.903	22.91	23.18	43.13	1.91	2062.4
16	19-May-05	61	140	35.1	3	32.927	22.42	22.71	42.29	1.77	2073.1
17	23-May-05	65	144	36.7	3	32.925	21.75	22.02	41.74	1.84	2105.8
18	27-May-05	69	148	35.4	3	32.963	23.23	23.47	45.66	1.93	1935.6
19	31-May-05	73	152	34.6	3	32.905	22.78	23.04	44.38	1.88	2073.7
20	04-Jun-05	77	156	36.1	4	32.887	22.47	22.74	43.93	1.91	2084.4
21	08-Jun-05	81	160	35.7	4	32.893	21.69	21.98	43.05	1.84	2080.5
22	12-Jun-05	85	164	34.8	4	32.880	21.71	21.99	42.88	1.83	2080.5
23	16-Jun-05	89	168	35.3	4	32.878	22.11	22.36	43.93	1.85	2087.9
24	20-Jun-05	93	172	35.3	4	32.915	22.21	22.44	45.09	1.88	2081.3
25	24-Jun-05	97	176	35.6	4	32.921	22.64	22.89	45.58	1.93	2095.7
26	28-Jun-05	101	180	35.7	4	32.896	21.60	21.85	44.48	1.86	2095.0
27	02-Jul-05	105	184	35.2	6	32.883	19.35	19.62	38.41	1.71	2069.1
28	06-Jul-05	109	188	35.8	6	32.860	17.63	17.89	30.33	1.69	2047.5
29	10-Jul-05	113	192	36.1	6	32.863	18.87	19.10	37.95	1.77	2061.2
30	14-Jul-05	117	196	34.6	6	32.859	18.92	19.15	39.50	1.75	2071.2
31	18-Jul-05	121	200	35.4	5	32.853	19.18	19.42	37.58	N.D.	1959.0
32	22-Jul-05	125	204	35.6	6	32.879	19.22	19.54	37.04	N.D.	2065.7
33	26-Jul-05	129	208	35.1	5	32.937	21.66	21.92	42.36	1.97	2081.5
34	30-Jul-05	133	212	34.9	6	32.849	17.06	17.32	30.30	1.77	2052.2
35	03-Aug-05	137	216	34.9	7	32.841	16.26	16.52	26.72	1.66	2057.4
36	07-Aug-05	141	220	35.7	5	N.S.	N.S.	N.S.	N.S.	N.S.	N.S.
37	11-Aug-05	145	224	34.6	4	32.982	19.57	19.85	37.25	1.76	2035.5
38	15-Aug-05	149	228	35.0	5	32.955	19.26	19.50	37.13	N.D.	2049.9
39	19-Aug-05	153	232	35.0	7	32.910	17.37	17.62	28.93	N.D.	2024.3
40	23-Aug-05	157	236	34.6	5	32.965	19.04	19.30	36.36	1.77	2056.7
41	27-Aug-05	161	240	34.8	6	32.849	15.52	15.74	23.13	1.32	1976.7
42	31-Aug-05	165	244	34.8	7	32.887	18.16	18.42	32.12	N.D.	2007.2
43	04-Sep-05	169	248	34.6	7	32.853	16.81	17.07	24.60	1.71	2058.1
44	08-Sep-05	173	252	35.7	8	32.805	14.42	14.67	17.61	1.54	2038.6
45	12-Sep-05	177	256	34.2	11	32.777	13.05	13.25	15.65	N.D.	1967.1
46	16-Sep-05	181	260	34.9	10	N.S.	N.S.	N.S.	N.S.	N.S.	N.S.
47	20-Sep-05	185	264	36.1	10	32.955	12.69	12.91	21.54	1.28	1987.1

centrations was better during phase II than phase I. Correlation coefficients (r) during phase II were 0.90 for NO_x, 0.88 for $Si(OH)_4$, and 0.84 for PO_4. During phase I the coefficients were 0.55 for NO_x, 0.55 for $Si(OH)_4$, and 0.37 for PO_4. These values can be attributed to the fact that nutrients behaved non-conservatively, unlike salinity, during phase I, while they behaved conservatively, like salinity, during phase II. The decrease in nutrient concentrations from late spring to late summer can be explained in terms of biological activity in the mixed layer, and the nutrient increases from late autumn to late winter resulted from physical processes; i.e. the expansion of the mixed layer supplied nutrients from deeper water (>100 m).

3.2.4 DIC

N-DIC also shows a seasonal decrease from April to September 2005 and an increase from October 2005 to April 2006 (Fig. 4(d)). N-DIC in RAS samples collected

Table 2. (continued).

(Phase II) Deployment date: 25-Sep-05; Recovery date: 31-May-06; Position: 47°00′ N, 159°58′ E; Water depth: 5206 m

S/N	Sampling date	Experimental days	Julian days	RAS depth (m)	Water temp. (deg-C)	Salinity	NO_3 (μmol kg^{-1})	NO_x (μmol kg^{-1})	$Si(OH)_4$ (μmol kg^{-1})	PO_4 (μmol kg^{-1})	DIC (μmol kg^{-1})
48	01-Oct-05	196	275	38.70	11	32.855	12.86	13.06	18.30	1.27	2035.7
49	05-Oct-05	200	279	38.45	11	32.772	12.78	12.96	16.45	1.28	2032.2
50	09-Oct-05	204	283	48.80	10	32.707	13.41	13.63	14.23	1.31	2029.9
51	13-Oct-05	208	287	38.35	10	N.S.	N.S.	N.S.	N.S.	N.S.	N.S.
52	17-Oct-05	212	291	41.70	10	32.614	11.90	12.12	14.66	1.22	2025.2
53	21-Oct-05	216	295	37.55	9	32.552	11.21	11.42	14.42	1.17	2020.1
54	25-Oct-05	220	299	41.50	9	32.567	12.25	12.50	16.38	1.25	2029.0
55	29-Oct-05	224	303	44.60	8	32.506	12.47	12.80	17.62	1.27	2028.1
56	02-Nov-05	228	307	43.45	8	32.512	12.65	13.01	17.98	1.33	2026.0
57	06-Nov-05	232	311	39.65	8	32.531	12.89	13.24	18.44	1.31	2028.5
58	10-Nov-05	236	315	38.75	8	32.554	13.19	13.51	17.98	1.32	2028.9
59	14-Nov-05	240	319	52.60	9	32.707	13.90	14.20	18.59	1.37	2037.9
60	18-Nov-05	244	323	38.40	9	32.740	14.25	14.59	18.51	1.38	2040.3
61	22-Nov-05	248	327	45.20	9	32.725	13.96	14.29	18.17	1.36	2031.7
62	26-Nov-05	252	331	49.90	8	32.682	13.84	14.17	18.37	1.37	2034.6
63	30-Nov-05	256	335	42.20	7	N.S.	N.S.	N.S.	N.S.	N.S.	N.S.
64	04-Dec-05	260	339	45.25	6	32.556	14.18	14.46	19.80	N.D.	2023.2
65	08-Dec-05	264	343	41.95	6	32.609	14.84	15.11	20.09	N.D.	2022.9
66	12-Dec-05	268	347	50.05	5	32.625	15.80	16.06	22.91	N.D.	2029.5
67	16-Dec-05	272	351	49.95	6	32.671	15.81	16.08	23.27	1.42	2037.3
68	20-Dec-05	276	355	50.50	5	32.675	16.46	16.71	24.54	1.43	2035.0
69	28-Dec-05	284	363	37.90	4	32.693	17.93	18.14	27.24	1.57	2041.0
70	05-Jan-06	292	371	40.05	4	32.765	19.28	19.47	29.91	1.66	2053.3
71	13-Jan-06	300	379	37.30	3	32.821	20.34	20.53	31.99	1.59	2063.4
72	21-Jan-06	308	387	36.35	3	32.810	19.95	20.12	31.48	1.69	2057.5
73	29-Jan-06	316	395	39.50	3	32.789	21.55	21.75	33.89	N.D.	2053.7
74	06-Feb-06	324	403	35.90	2	32.895	22.14	22.32	36.38	1.80	2078.6
75	14-Feb-06	332	411	36.25	2	32.910	22.47	22.65	37.11	1.84	2075.1
76	22-Feb-06	340	419	35.65	2	32.930	22.97	23.15	38.33	N.D.	2081.6
77	02-Mar-06	348	427	36.60	2	32.919	23.00	23.20	38.63	1.84	2083.9
78	10-Mar-06	356	435	37.80	2	32.923	23.17	23.38	38.18	N.D.	2083.0
79	18-Mar-06	364	443	53.50	2	32.952	24.00	24.22	39.47	N.D.	2088.6
80	26-Mar-06	372	451	38.90	2	32.958	24.24	24.46	40.65	N.D.	2087.5
81	03-Apr-06	380	459	40.25	2	32.944	23.89	24.11	40.80	N.D.	2083.7
82	11-Apr-06	388	467	37.45	2	32.923	24.03	24.23	37.70	N.D.	2072.9
83	15-Apr-06	392	471	38.70	2	32.930	24.13	24.33	36.61	N.D.	2074.1
84	19-Apr-06	396	475	38.00	2	N.S.	N.S.	N.S.	N.S.	N.S.	N.S.
85	23-Apr-06	400	479	36.40	2	32.929	24.17	24.39	40.96	N.D.	2082.5
86	27-Apr-06	404	483	37.05	2	32.921	23.94	24.18	42.10	1.96	2092.2
87	01-May-06	408	487	38.00	2	32.917	23.71	23.96	40.98	1.98	2096.5
88	05-May-06	412	491	35.30	2	32.913	23.67	23.91	41.95	1.95	2088.4
89	09-May-06	416	495	36.10	2	32.934	23.59	23.82	42.19	1.96	2053.9
90	13-May-06	420	499	36.15	3	32.913	23.66	23.91	40.81	N.D.	2072.3
91	17-May-06	424	503	35.60	3	32.908	23.18	23.44	39.81	1.92	2079.8
92	21-May-06	428	507	38.00	3	32.903	23.50	23.74	40.45	N.D.	2068.5
93	25-May-06	432	511	35.30	3	32.874	23.26	23.50	40.76	1.87	2071.9
94	29-May-06	436	515	38.55	3	33.100	22.86	23.10	40.92	1.92	2087.3

in the early parts of phase I (March and April 2005) and phase II (October and November 2006) agreed with hydrocast N-DIC data. However, the variation in N-DIC was large during phase I, and low N-DIC concentrations (less than 2030 μmol kg^{-1}) were often observed. Based on climatological data, the annual minimum N-DIC concentration at station K2 is at least 2030 μmol kg^{-1}, which is usually observed at the near surface in autumn. During phase II, concentrations of N-DIC from RAS samples were consistently lower than climatological data.

4. Discussion

4.1 Low DIC and PO_4 in RAS samples

Observed N-DIC values from RAS samples were substantially lower than climatological N-DIC values, with some exceptions, and in some RAS samples there were problems with PO_4 measurement. Sample storage was probably not the cause, since we had verified that preservation with $HgCl_2$ permitted measurements of nutrients and DIC after long periods of storage (see Sub-

section 2.3).

The low DIC values were not accompanied by decreases of N-NO_x and N-$Si(OH)_4$. In the ocean, the biogenic production of $CaCO_3$ and gas exchange with the atmosphere reduces DIC without a decrease in nutrient concentrations. However, these are unlikely explanations for the variations observed because the biogenic production of $CaCO_3$ is not predominant in the WSG, and CO_2 exchange should not occur so rapidly at the RAS depth (approximately 35 m), as is evident in the sudden decreases of N-DIC (Fig. 4(d)). In addition, these mechanisms cannot explain the systematic reduction of N-DIC during phase II. Authigenic $CaCO_3$ production in the RAS sampling bag is another possibility, but the degree of supersaturation in seawater is estimated to be at most 2.5 for calcite and 1.5 for aragonite, which is too low for authigenic $CaCO_3$ production.

We attribute the unexpected low N-DIC concentrations to depletion of DIC by CO_2 degassing from the RAS seawater sample, possibly caused by a decrease in pH from the HCl solution used for pre-washing the sampling inlet. Although this HCl solution was subsequently rinsed with ambient seawater before sampling, and sampling started 5 minutes after the HCl flush, some HCl might have remained in the sampling line, or sampled seawater might have been affected by HCl. Another possibility is that degassing occurred after recovery, especially for seawater samples collected during phase II. RAS samples from phase II were kept onboard at room temperature (approximately 15°C) for one month until onboard chemical analysis. Degassing during storage might have occurred, although RAS samples were sealed with plastic caps to prevent interaction with the atmosphere. Degassing could have also resulted from pressure reduction after sampling. The RAS system collected seawater samples using a pressure gradient caused by withdrawing water from the acrylic container holding the sample bag. However, if the intake rate of the seawater sample was slower than the exhaust rate of high saline seawater in an acrylic container, the pressure in the sample bag would be higher than that of the surrounding high saline water after valves (e.g. valve P3 at both sides in Fig. 2(b)) closed and the pump stopped, resulting in degassing within the sample bag until pressure was equalized

Thus, the usefulness of the RAS for collecting seawater samples for DIC measurements is questionable at this time. To improve usefulness in the future, the use of a copper barrier for effective anti-biofouling (Dickey *et al*., 2003; Manov *et al*., 2004; Honda *et al*., 2006) might be more appropriate than HCl, and DIC measurements should be conducted as soon as possible after sample recovery.

Problems with PO_4 measurements could have been caused by incomplete reduction of phosphomolybdic acid to phosphomolybdous acid (i.e. molybdenum blue), by the reducing agent ascorbic acid. Possible interfering substances were $HgCl_2$ and HCl. Eberlein and Kattner (1987) reported that $HgCl_2$ and HCl would cause interference in the total phosphorus measurements because ascorbic acid reacts with free chlorine and is thereby unable to reduce the phosphomolybdic acid. $HgCl_2$ can probably be eliminated as the cause of the problem because all RAS samples were preserved with $HgCl_2$, but only about 20% had problems with PO_4 analysis, and Kattner (1999), as well as our test of sample preservation, demonstrated that use of $HgCl_2$ is not problematic for PO_4 measurement. Contamination of RAS samples by HCl might affect measurements of PO_4 by changing the pH of the seawater sample. However, HCl contamination would also cause lowered DIC measurements, which were not always evident in the problematic samples. Other possible causes, such as the effect of suspended particles or colloidal substances in RAS samples, should be investigated to improve the measurement of PO_4 concentrations.

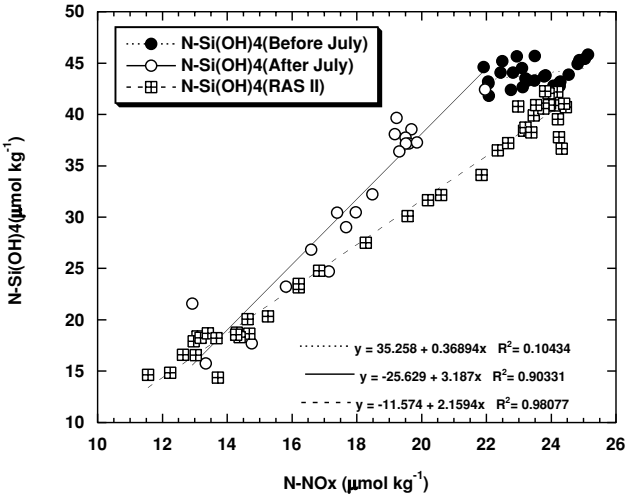

Fig. 5. Relationship between normalized NO_x (N-NO_x) and $Si(OH)_4$ (N-$Si(OH)_4$). Data are divided into three groups: closed circles with dotted regression line, data from before the end of June 2005; open circles with solid regression line, from July through September 2005; squares with broken regression line, after October 2005 (phase II).

4.2 Application of RAS data to oceanography

4.2.1 The ratio of changes in $Si(OH)_4$ and NO_x

Data comparing N-$Si(OH)_4$ with N-NO_x were divided into three groups: data from before and after the end of June 2005 during phase I, and data from phase II (Fig. 5). Before the end of June 2005, the ratio of changes of N-$Si(OH)_4$ to N-NO_x ($\Delta Si/\Delta N$) was approximately 0.4, without a statistically significant correlation. However, $\Delta Si/$

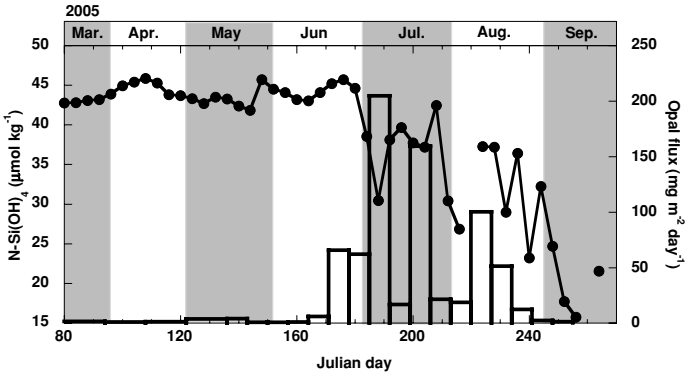

Fig. 6. N-$Si(OH)_4$ concentrations between 20 March 2005 and 20 September 2005 (line graph) and biogenic opal flux at 150 m observed by sediment trap (bar graph, Honda *et al*., 2006).

ΔN between July and September 2005 was estimated to be 3.2 with good correlation (r^2 = 0.9). This increase in ΔSi/ΔN could be caused by: (1) predominance of diatoms after the end of July; (2) an increase in the diatom Si/N uptake ratio which occurs under any type of stress, such as lower or higher temperature, light limitation, or iron limitation; or (3) preferential decomposition of particulate inorganic nitrogen (PIN) (reviewed by Saito *et al*., 2002).

The first cause is the most likely, based on the dramatic increase in biogenic opal flux observed in sediment trap samples at 150 m after late June. Before this, opal flux had been very low (Fig. 6). The large decrease of dissolved $Si(OH)_4$ was accompanied not only by the increase in opal flux, but also by an increase of phytoplankton abundance and primary productivity in the euphotic layer, based on optical observation (Honda *et al*., 2006). This evidence indicates that nutrients and DIC assimilated by phytoplankton, primarily diatoms, in the euphotic layer were quickly transported vertically to at least 150 m in the ocean interior.

4.2.2 Estimation of annual new production

One method for assessing the level of activity of the biological pump is to determine of magnitude of the seasonal NO_x drawdown and to estimate annual new production (Eppley, 1989; Codispoti, 1989; Lourey and Trull, 2001; Wong *et al*., 2002a, b). Launchi and Najjar (2000) estimated annual global new production in the upper 100 m using the annual minimum NO_x data observed at the surface in the late August and data from 100 m in winter as the annual maximum. On the other hand, Wong *et al*. (2002b) estimated annual new production for the North Pacific using seasonal surface nutrient data observed by ships of opportunity and assuming that the surface mixed layer is 50 m thick.

Even though in this study the RAS collected seawater samples at one depth, this depth was generally located in or very close to the surface MLD (Fig. 3(a)). The RAS

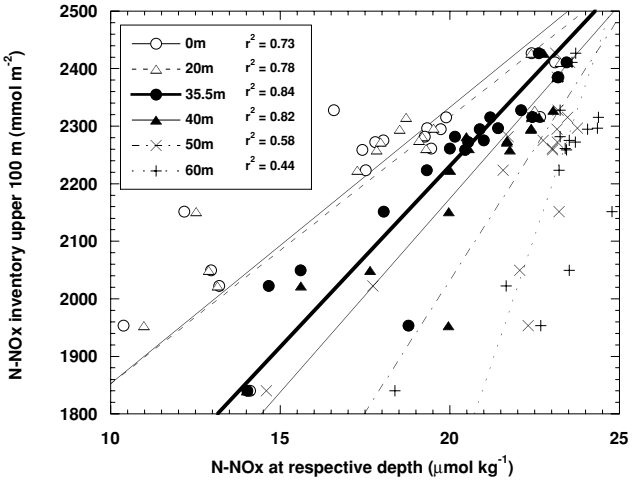

Fig. 7. Relationship between N-NO_x at 35.5 m (RAS depth during phase I) and N-NO_x inventory (total N-NO_x) integrated over the upper 100 m based on climatological data (solid circles and heavy solid line). Correlation coefficient (r^2) is 0.84. Data also shown for depths of 0 m (open circles, r^2 = 0.73), 20 m (open triangles, r^2 = 0.78), 40 m (solid triangles, r^2 = 0.82), 50 m ("X" signs, r^2 = 0.58) and 60 m ("plus" signs, r^2 = 0.44).

data provide annual maximum and minimum NO_x values in the mixed layer and therefore RAS data from this study can contribute to the estimation of annual new production. The determination of new production requires an estimate of the seasonal drawdown of nutrients integrated over the upper 100 m of the water column, which is the depth of the permanent halocline or pycnocline in the WSG (Favorite *et al*., 1976) and of the chlorophyll-*a* depletion layer at station K2 (Kawakami, unpublished data). We estimated the seasonal drawdown of integrated nutrients (the nutrient inventory) in the upper 100 m using

only data from 35.5 m, which was the approximate average RAS depth during phase I.

We used previously observed climatological data to derive an empirical equation to estimate integrated nutrients in the upper 100 m using nutrient data from 35.5 m, although at low N-NO_x values, there was a larger deviation from the derived regression line because these low values correspond to samples from below the mixed layer (Fig. 7). We applied this empirical equation to the maximum and minimum RAS nutrient values and assumed that biological drawdown of N-DIC follows the Redfield ratio ($\Delta C/\Delta N = 6.6$). We estimated the annual new production (the difference between maximum inventory estimated with maximum N-NO_x observed in April 2005 and minimum inventory with minimum N-NO_x observed in October 2005) as approximately 156 mg-C $m^{-2}day^{-1}$ or 57 g-C $m^{-2}yr^{-1}$. This estimate is slightly higher than estimates by Midorikawa *et al*. (2002) (approximately 33 g-C $m^{-2}yr^{-1}$) and Andreev *et al*. (2002) (approximately 37 g-C $m^{-2}yr^{-1}$), and is comparable to those by Wong *et al*. (2002b) (57–88 g-C $m^{-2}yr^{-1}$; average, 67 g-C $m^{-2}yr^{-1}$) and Launchi and Najjar (2000) (40–60 g-C $m^{-2}yr^{-1}$).

We also investigated the relationship between the N-NO_x inventory in the upper 100 m and N-NO_x concentrations at various discreet depths (0–100 m) other than 35.5 m (Fig. 7) and verified that N-NO_x values at depths shallower than 40 m are well correlated with the N-NO_x inventory in the upper 100 m ($r^2 > 0.7$), while N-NO_x values from depths greater than 60 m do not show good correlation ($r^2 < 0.5$). The N-NO_x inventory in the upper 100 m was more closely correlated with N-NO_x concentrations at 35.5 m and 40 m ($r^2 > 0.8$, $p < 0.0001$) than at the surface ($r^2 = 0.73$) (Fig. 7). Therefore, annual new production in the WSG can be accurately estimated from RAS data obtained from a single depth, provided that depth is shallower than 40 m.

5. Concluding Remarks

The determination of nutrient and DIC concentrations is essential for understanding biological pump processes and variability, especially in the northwestern North Pacific Ocean, where there are great seasonal changes in biological activity. However, ordinary shipboard sampling limits the temporal resolution of time-series observations used for biogeochemical studies.

This study confirms the utility of automated water sampling systems for time-series observation of NO_x and $Si(OH)_4$. It remains difficult to moor instruments near the sea surface in the northwestern North Pacific because of rough seas, with waves exceeding 20 m in height, and the presence of ships with drafts greater than 10 m. However, combining satellite and sediment trap data with data from an RAS deployed at subsurface levels will contribute greatly to quantifying seasonal variability in nutrients and biological pump activity. Moreover, coupling RAS data with mathematical simulations will reveal more precisely the variability of the biological pump and CO_2 exchange between the atmosphere and ocean.

Acknowledgements

We express our appreciation to S. Honjo of the Woods Hole Oceanographic Institution (WHOI) for his efforts to promote time-series observations with mooring systems. We especially thank K. Hayashi of Marine Works Japan, Co. (MWJ), who maintained the RAS system and established procedures for the chemical analysis of RAS sample. We are grateful to J. Kemp and his team of WHOI and T. Idai of MWJ for their mooring work and maintenance of the mooring system. We appreciate K. Doherty of McLane Research Laboratories, Inc. for the design of the RAS. Masters M. Akamine and Y. Kita and the officers and crews of the R/V *MIRAI*, and the onboard analytical team from MWJ, including J. Hamanaka, K. Sato, A. Takeuchi, M. Kamata, M. Moro and F. Shibata, provided us with their expertise. K. Sasaoka, M. Wakita and Y. Nakano of Japan Agency for Marine-Earth Science and Technology (JAMSTEC) provided satellite data, approved climatological data and estimates of $CaCO_3$ supersaturation rates for RAS samples, respectively. We thank K. Buesseler of WHOI and the VERTIGO group for their permission to use unpublished data. Finally, we acknowledge reviewers, P. Brewer, Y. Nakaguchi and T. Gamo, for their constructive and suggestive comments.

Appendix

Abbreviations used in text and captions are as follows:

AFP:	Acid Flush Path
AVHRR:	Advanced Very High Resolution Radiometer
DIC:	Dissolved Inorganic Carbon
MLD:	Mixed Layer Depth
RAS:	Remotely Access Sampler
SST:	Sea Surface Temperature
VERTIGO:	VERtical Transport In the Global Ocean
WFP:	Water Flush Path
WSG:	Western Subarctic Gyre

References

Anderson, L. A. and J. L. Sarmiento (1994): Redfield ratios of remineralization determined by nutrient data analysis. *Global Biogeochem. Cycles*, **8**, 65–80.

Andreev, A., M. Kusakabe, M. Honda, A. Murata and C. Saito (2002): Vertical fluxes of nutrients and carbon through the halocline in the western subarctic Gyre calculated by mass balance. *Deep-Sea Res. II*, **49**, 5577–5593.

Aoyama, M. (2005): 3.4 Nutrients. p. 128. In *WHP P6, A10, I3/I4 Revisit Data Book: Blue Earth Global Expedition 2003*

(BEAGLE2003) Vol. 2, ed. by H. Uchida and M. Fukasawa, Aiwa Printing, Tokyo.
Banse, K. and D. C. English (1999): Comparing phytoplankton seasonality in the eastern and western Subarctic Pacific and the western Bering Sea. *Prog. Oceanogr.*, **43**, 235–288.
Behrenfeld, M. J., E. Boss, D. A. Siegel and D. M. Shea (2005): Carbon-based ocean productivity and phytoplankton physiology from space. *Global Biogeochem. Cycles*, **19**(1), GB100610.1029/2004GB002299.
Bell, J., J. Betts and E. Boyle (2002): MITESS: a moored *in situ* trace element serial sampler for deep-sea moorings. *Deep-Sea Res. I*, **49**, 2103–2118.
Buesseler, K. O., J. Bishop, P. Boyd, K. Casciotti, F. Dehairs, C. Lamborg, D. Siegel, M. W. Silver, D. Steinberg, S. Saitoh, T. Trull, J. R. Valdes and B. Van Mooy (2006): What we know from VERTIGO - OS22H-02. *Abstracts of 2006 AGU Ocean Sciences Meeting-Honolulu.*
Campbell, J. and 22 co-authors (2002): Comparisons of algorithms for estimating ocean primary production from surface chlorophyll, temperature, and irradiance. *Global Biogeochem. Cycles*, **16**(10), doi: 10.1029/2001GB001444.
Codispoti, L. A. (1989): Phosphorous vs. nitrogen limitation of new and export production. p. 377–394. In *Productivity of the Ocean: Present and Past*, ed. by W. H. Berger, V. S. Smetacek and G. Wefer, Wiley, New York.
Conte, M. H., N. Ralph and E. Ross (2001): Seasonal and interannual variability in deep ocean particle fluxes at the Oceanic Flux Program/Bermuda Atlantic Time-series (BATS) site in the western Sargasso Sea near Bermuda. *Deep-Sea Res. II*, **48**, 1471–1505.
Conte, M. H., T. D. Dickey, J. C. Weber, R. J. Johnson and A. H. Knap (2003): Transient physical forcing of pulsed export of bioreactive organic material to the deep Sargasso Sea. *Deep-Sea Res. I*, **50**(10–11), 1157–1187.
Dickey, T., J. Marra, R. Weller, D. Sigurdson, C. Langdon and C. Kinkade (1998): Time-series of bio-optical and physical properties in the Arabian Sea: October 1994–October 1995. *Deep-Sea Res. II*, **45**, 2001–2025.
Dickey, T., S. Zedler, D. Frye, H. Jannasch, D. Manov, D. Sigurdson, J. D. McNeil, L. Dobeck, X. Yu, T. Gilboy, C. Bravo, S. C. Doney, D. A. Siegel and N. Nelson (2001): Physical and biogeochemical variability from hours to years at the Bermuda Testbed Mooring site: June 1994–March 1998. *Deep-Sea Res. II*, **48**, 2105–2131.
Dickey, T., C. Moore and O-SCOPE Group (2003): New sensors monitor bio-optical/biogeochemical ocean changes. *Sea Tech.*, **44**, 17–24.
Dickey, T., M. R. Lewis and G. C. Chang (2006): Optical oceanography: recent advances and future directions using global remote sensing and in situ observations. *Rev. Geophys.*, **44**(1), RG1001, 10.1029/2003RG000148.
DOE (1994): *Handbook of Methods for the Analysis of the Various Parameters of the Carbon Dioxide System in Seawater*, ed. by A. G. Dickson and C. Goyet, Version 2, Carbon Dioxide Information Center, Report ORNL/CDIAC-74, Oak Ridge National Laboratory, Oak Ridge, TN, U.S.A.
Eberlein, K. and G. Kattner (1987): Automatic method for the determination of ortho-phosphate and total dissolved phosphorus in the marine environment. *Fresenius 'Z. Anal. Chem.*, **326**, 354–357.
Eppley, R. W. (1989): New production: history, methods, and problem. p. 85–97. In *Productivity of the Ocean: Present and Past*, ed. by W. H. Berger, V. S. Smetacek and G. Wefer, Wiley, New York.
Falkowski, P. G., R. T. Barber and V. Smetacek (1998): Biogeochemical controls and feedbacks on ocean primary production. *Science*, **281**, 200–206.
Favorite, F., A. J. Dodimead and K. Nasu (1976): Oceanography of the Subarctic pacific Region, 1960–71. *Bull. Int. North Pacific Fishery Commission*, **33**, 1–187.
Harrison, P. J., P. W. Boyd, D. E. Varela, S. Takeda, A. Shiomoto and T. Odate (1999): Comparison of factors controlling phytoplankton productivity in the NE and NW Subarctic Pacific gyres. *Prog. Oceanogr.*, **43**, 205–234.
Harrison, P. J., F. A. Whitney, A. Tsuda, H. Saito and K. Tadokoro (2004): Nutrient and plankton dynamics in the NE and NW gyres of the Subarctic Pacific ocean. *J. Oceanogr.*, **60**, 93–117.
Heinze, C. (2004): Simulating oceanic $CaCO_3$ export production in the greenhouse. *Geophys. Res. Lett.*, **31**, L16308, doi:10.1029/2004GL020613.
Honda, M. C. (2005): Time-series observation for study of CO_2 cycle in the North Pacific with mooring systems. *Navigation*, **163**, 67–77 (in Japanese).
Honda, M. C., K. Imai, Y. Nojiri, F. Hoshi, T. Sugawara and M. Kusakabe (2002): The biological pump in the northwestern North Pacific based on fluxes and major component of particulate matter obtained by sediment trap experiments (1997–2000). *Deep-Sea Res. II*, **49**, 5595–5626.
Honda, M. C., H. Kawakami, K. Sasaoka, S. Watanabe and T. Dickey (2006): Quick transport of primary produced organic carbon to the ocean interior. *Geophys. Res. Lett.*, **33**, L16603, doi:10.1029/2006GL026466.
Honjo, S. (1996): Fluxes of particles to the interior of the open ocean. p. 91–154. In *Particle Flux in the Ocean, SCOPE 57*, ed. by V. Ittekkot, P. Schafer, S. Honjo and P. J. Depetris, John Wiley & Sons, New York.
Idai, T., M. Honda, S. Honjo and J. Kemp (2005): Mooring systems for time-series observation for biogeochemistry in the northwestern North Pacific. *JAMSTEC Rep. Res. Dev.*, **1**, 73–91.
Imai, K., Y. Nojiri, N. Tsurushima and T. Saino (2002): Time series of seasonal variation of primary productivity at station KNOT (44°N, 155°E) in the sub-arctic western North Pacific. *Deep-Sea Res. II*, **49**, 5395–5408.
Ishii, M., H. Y. Inoue, H. Matsueda and E. Tanoue (1998): Close coupling between seasonal biological production and dynamics of dissolved inorganic carbon in the Indian Ocean section and the western Pacific ocean sector of the Antarctic ocean. *Deep-Sea Res. I*, **45**, 1187–1209.
Karl, D. M., J. R. Christian, J. E. Dore, D. V. Hebel, R. M. Letelier, L. M. Tupas and C. D. Winn (1996): Seasonal and interannual variability in primary production and particle flux at station ALOHA. *Deep-Sea Res.*, **43**, 539–568.
Karl, D. M., J. E. Dore, R. Lukas, A. Michaels, N. R. Bates and A. Knap (2001): Building the long-term picture: The U.S.JGOFS Time-series programs. *Oceanogr.*, **14**(4), 6–17.
Kattner, G. (1999): Storage of dissolved inorganic nutrients in

seawater: poisoning with mercuric chloride. *Mar. Chem.*, **67**, 61–66.

Launchi, F. and R. G. Najjar (2000): A global monthly climatology of phosphate, nitrate, and silicate in the upper ocean: Spring-summer export production and shallow remineralization. *Global Biogeochem. Cycles*, **14**, 957–977.

Lourey, M. and T. W. Trull (2001): Seasonal nutrient depletion and carbon export in the Subantarctic and Polar Frontal Zones of the Southern Ocean south of Australia. *J. Geophys. Res.*, **106**(C12), 31463–31487.

Manov, D., G. Chang and T. Dickey (2004): Methods for reducing biofouling on moored optical sensors. *J. Atoms. Oceanic Technol.*, **21**, 957–967.

Midorikawa, T., T. Umeda, N. Hiraishi, K. Ogawa, K. Nemoto, N. Kudo and M. Ishii (2002): Estimation of seasonal net community production and air-sea CO_2 flux based on the carbon budget above the temperature minimum layer in the western subarctic North Pacific. *Deep-Sea Res. I*, **49**, 339–362.

Mochizuki, M., N. Shiga, M. Saito, K. Imai and Y. Nojiri (2002): Seasonal changes in nutrients, chlorophyll *a* and the phytoplankton assemblage of the western subarctic gyre in the Pacific Ocean. *Deep-Sea Res. II*, **49**, 5421–5439.

Murphy, J. and J. P. Riley (1961): Modified single solution method for the determination of phosphate in natural water. *Anal. Chem. Acta*, **27**, 31–36.

Orr, J. C., V. J. Fabry, O. Aumont, L. Bopp, S. C. Doney, R. A. Feely, A. Gnanadesikan, N. Gruber, A. Ishida, F. Joos, R. M. Key, K. Lindsay, E. Maier-Reimer, R. Matear, P. Monfray, A. Mouchet, R. G. Najjar, G-K. Plattner, K. B. Rodgers, C. L. Sabine, J. L. Sarmiento, R. Schlitzer, R. D. Slater, I. J. Totterdell, M-F. Weirig, Y. Yamanaka and A. Yool (2005): Anthropogenic ocean acidification over the twenty-first century and its impact on calcifying organisms. *Nature*, **437**, 681–686.

Redfield, A. C., B. H. Ketchum and F. A. Richards (1963): The influences of organisms on the composition of seawater. p. 26–77. In *The Sea*, ed. by M. H. Hill, Wiley-Interscience, New York.

Saito, H., A. Tsuda and H. Kasai (2002): Nutrient and plankton dynamics in the Oyashio region of the western subarctic Pacific Ocean. *Deep-Sea Res. II*, **49**, 5463–5486.

Sarmiento, J. L. and C. LeQuere (1996): Oceanic carbon dioxide uptake in a model of century-scale global warming. *Science*, **274**, 1346–1350.

Sigman, D. M. and E. A. Boyle (2000): Glacial/Interglacial variations in atmospheric carbon dioxide. *Nature*, **407**, 859–869.

Takahashi, T., S. C. Sutherland, C. Sweeny, A. Poisson, N. Metzl, B. Tilbrook, N. Bates, R. Wanninkhof, R. A. Feely, C. Sabine, J. Olafsson and Y. Nojiri (2002): Global sea-air CO_2 flux based on climatological surface ocean pCO_2, and seasonal biological and temperature effects. *Deep-Sea Res. II*, **49**, 1601–1622.

Tsurushima, N., Y. Nojiri, K. Imai and S. Watanabe (2002): Seasonal variations of carbon dioxide system and nutrients in the surface mixed layer at station KNOT (44°N, 155°E) in the subarctic western North Pacific. *Deep-Sea Res. II*, **49**, 5377–5394.

Volk, T. and M. I. Hoffert (1985): Ocean carbon pumps: Analysis of relative strengths and efficiencies in ocean-driven atmospheric CO_2 changes. p. 99–110. In *The Carbon Cycle and Atmospheric CO_2: In Natural Variations Archean to Present*, ed. by E. Sundquist and W.S. Broecker, AGU, Washington, D.C.

Wong, C. S., N. A. D. Waser, Y. Nojiri, F. A. Whitney, J. S. Page and J. Zeng (2002a): Seasonal cycles of nutrients and dissolved inorganic carbon at high and mid latitudes in the North Pacific Ocean during the *skaugran* cruises: determination of new production and nutrient uptake ratios. *Deep-Sea Res. II*, **49**, 5317–5338.

Wong, C. S., N. A. D. Waser, Y. Nojiri, Wm. K. Johnson, F. A. Whitney, J. S. C. Page and J. Zeng (2002b): Seasonal and interannual variability in the distribution of surface nutrients and dissolved inorganic carbon in the northern North Pacific: Influence of El Niño. *J. Oceanogr.*, **58**, 227–243.